

Amine-induced growth of an In₂O₃ shell on colloidal InP nanocrystals†

Myriam Protière^a and Peter Reiss^{*b}

Received (in Cambridge, UK) 24th January 2007, Accepted 22nd February 2007

First published as an Advance Article on the web 13th March 2007

DOI: 10.1039/b701092c

A simple and rapid method for the growth of an In₂O₃ shell on colloidal InP nanocrystals is described, increasing their fluorescence efficiency by one order of magnitude.

Indium phosphide nanocrystals are potentially an attractive alternative to CdSe or CdTe ones due to their size-dependent emission in the visible and near infrared spectral range combined with the lower toxicity of indium with respect to cadmium. In the last decade, several robust methods for the chemical synthesis of colloidal InP nanocrystals have been developed.^{1–4} On the other hand, it still remains a challenge to achieve significant emission efficiencies with this system. The low fluorescence quantum yield (Q.Y.) observed for as-synthesized InP nanocrystals (< 0.1%) has been attributed to dangling bonds of surface phosphorus atoms acting as trap states for photo-generated electrons.² An elegant way to passivate these trap states and to increase the Q.Y. to values of 25–40% is photo-assisted etching by HF.^{1,2} Nevertheless the nanocrystals' optical properties are still sensitive to subsequent functionalization of their surface, which is required for most applications. In the case of II–VI semiconductor nanocrystals, the coating of their surface with a shell of a higher bandgap semiconductor has proven to be the method of choice to overcome this problem.^{5–7} Much less information can be found concerning such core–shell systems based on InP. Haubold *et al.* used organometallic precursors to grow a ZnS shell on InP and observed a subsequent increase of the Q.Y. in a slow room temperature process to 15% after three days and to 23% after three weeks.⁸ In order to adjust the lattice parameters of the core and shell materials and to reduce strain-induced defects, Micic and coworkers developed a CdZnSe₂ shell leading to a fluorescence Q.Y. of 5–10%.⁹ Here we propose the coating of InP nanocrystals with an In₂O₃ shell, yielding fluorescence efficiencies in the same range. The most appealing feature of our synthesis method is its simplicity: the In₂O₃ shell growth takes place *in situ* without addition of any precursor to the reaction mixture containing the InP nanocrystals, and the reaction time is only 10 minutes. The shell growth is triggered by a specific amount of oleylamine (OA) initially added to the reaction mixture composed of indium acetate, myristic acid and octadecene (ODE).‡

Fig. 1 shows the UV–vis absorption and PL spectra of 3.1 nm InP nanocrystals (no amine added) and of the corresponding

7.2 nm InP–In₂O₃ core–shell particles (0.1 mmol of OA added). The absorption spectra of the samples with and without a shell exhibit two apparent differences (Fig. 1a). First, most probably as a consequence of the higher reaction temperature,¹⁰ the excitonic peak of the sample without a shell is shifted bathochromically by 26 nm with respect to the coated sample. Second, the In₂O₃ shell induces, as expected, an enhanced absorption in the UV part of the spectrum. The PL spectrum of the bare InP sample (Fig. 1b) exhibits, besides the peak corresponding to band edge emission at 597 nm, a significant amount of defect emission at longer wavelengths/lower energies. The growth of the In₂O₃ shell strongly diminishes the ratio of defect emission to band edge emission, while the emission linewidth of the predominant peak at 583 nm of 50–60 nm (FWHM) is not affected. Although this value is consistent with the reported linewidths of as-synthesized InP nanocrystals in the literature, it is rather high with respect to II–VI semiconductor nanocrystals (20–30 nm). The underlying broader size distribution of the InP nanocrystals reflects the intrinsic difficulty in synthesizing monodisperse samples with the reaction methods developed to date. Another difficulty arises from the very high sensitivity of indium toward oxidation, and therefore the strict utilisation of air-free working techniques is indispensable. It has been demonstrated that the Q.Y. is increased to values of *ca.* 0.5% by a surface oxide layer.¹¹ Importantly, we demonstrate here that the emission intensity is further enhanced by one order of magnitude through the growth of a thicker In₂O₃ shell. Using Rhodamine 6G as a standard, the measured room temperature PL Q.Y. reaches 6% if only band edge emission is considered, and 8% if the entire spectral range of emission is integrated (Fig. 1b).

In Fig. 2 TEM micrographs of the samples with and without a shell are compared. Despite the growth of the rather thick oxide shell in the second case, the size distribution increases only slightly from 12 to 14% and the particles' shape remains approximately

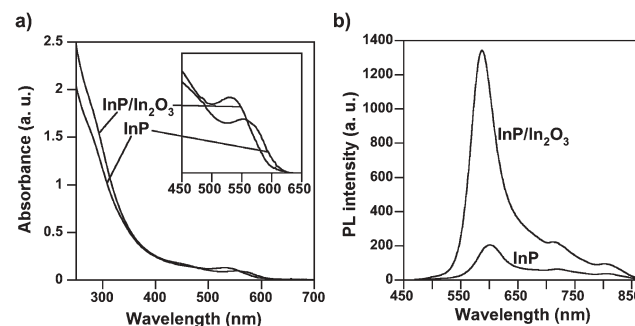


Fig. 1 UV–vis absorption (a) and photoluminescence (b) spectra of the prepared InP–In₂O₃ core–shell nanocrystals. The spectra of InP nanocrystals prepared without amine addition are shown for comparison. Both samples have the same absorption at the excitation wavelength (430 nm).

^aDRT/LITEN/DTNMI/2T, CEA Grenoble, 17 rue des Martyrs, 38054 Grenoble cedex 9, France

^bDSM/DRFMC/SPRAM (UMR 5819 CEA-CNRS-Université Joseph Fourier 1)/LEMOH, CEA Grenoble, 17 rue des Martyrs, 38054 Grenoble cedex 9, France. E-mail: peter.reiss@cea.fr;

Fax: +33 438 785113; Tel: +33 438 789719

† Electronic supplementary information (ESI) available: XRD and TEM data of a control sample with air introduced during the synthesis. See DOI: 10.1039/b701092c

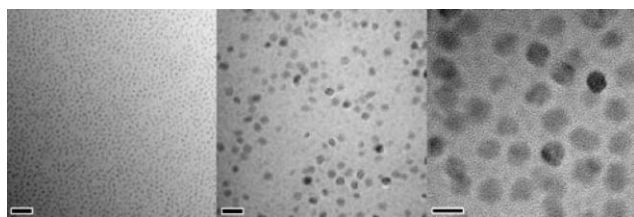


Fig. 2 TEM micrographs (JEOL 4000EX, 300 kV) of the prepared InP (left panel) and of the InP–In₂O₃ core–shell nanocrystals (middle and right panel). Scale bars: 20 nm, 20 nm, 10 nm (from left to right).

spherical. Structural characterization was carried out by means of powder X-ray diffraction. In the case of bare InP nanocrystals, the obtained diffraction pattern can be indexed as the zinc blende structure of InP (Fig. 3). The calculated crystallite size using the Scherrer formula is 2.6 nm, which is in fairly good agreement with the mean size determined from TEM (3.1 nm, Fig. 2 left panel). In the higher angle base of the broad 111 peak at 31°, a small signal attributed to the 200 reflection of InP can be detected at 36°. The intensity of this signal is strongly increased in the sample with the In₂O₃ shell due to the superposition with the predominant 222 reflection of indium oxide. Furthermore, additional peaks characteristic of bulk cubic In₂O₃ are visible in the diffractogram of the core–shell sample at 42° (400), and at 72° (622). The aforementioned superposition of diffraction patterns of both bulk crystalline structures clearly points to a core–shell structure. If alloying occurred, the peak positions would be expected to shift according to Vegard's law. The different valence states of the phosphide and oxide ions and the large lattice mismatch between InP and In₂O₃ are further arguments in favour of a core–shell structure. § The latter could also be at the origin of the limitation of the observed PL Q.Y. to values in the range of 5–10%. An analysis of the peak width of the core–shell sample gave results consistent with the TEM observations: the calculated size of the crystallites was 2.3 nm for InP and 6.6 nm for In₂O₃.

Indium oxide formation is induced by the addition of a controlled amount of primary amine (OA). ‡ A possible reaction mechanism is proposed in Scheme 1. In the reaction between indium myristate and P(TMS)₃, myristic acid anhydride molecules

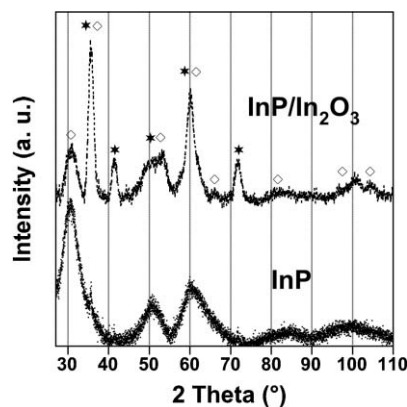
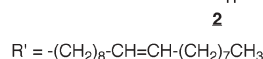
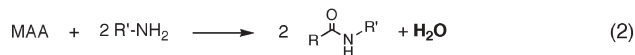
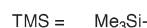
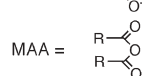
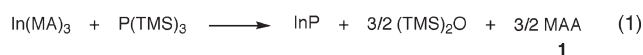


Fig. 3 Powder X-ray diffractogram (Philips X'Pert, Co source, 50 kV/35 mA) of the InP and InP–In₂O₃ core–shell nanocrystals. The peaks corresponding to bulk cubic InP and In₂O₃ are indexed with diamonds and stars, respectively.



Scheme 1 Partial reaction mechanism proposed for the formation of InP–In₂O₃ core–shell nanocrystals.

(MAA, **1**) are one of the by-products (Eq. 1). At elevated temperatures, OA can form amides (**2**) in a condensation reaction with MAA (Eq. 2). During this reaction water is released, which can hydrolyse remaining In precursor to form In₂O₃. Such a scenario is consistent with the facts that the In precursor is used in excess with respect to the P one and that the In₂O₃ formation can take place only after the InP one, resulting in a core–shell structure. A similar mechanism can be suspected in the recently reported synthesis of In₂O₃ nanoparticles by thermal decomposition of indium acetylacetonate in OA.¹² Nevertheless further analytical studies, in particular NMR spectroscopy, are necessary to confirm the proposed reaction pathway. Fig. 4a depicts the evolution of the PL Q.Y. with increasing quantity of added OA. A maximum is reached for an equimolar ratio of OA and In acetate. At the same time the molar ratio of OA : myristic acid is 1 : 3, implying that the myristate and/or myristate anhydride ligands are only partially transformed into the amide. This indicates that the addition of a specific well-controlled amount of OA is necessary to establish the delicate equilibrium within the reaction mixture, which allows for the homogeneous *in situ* coating of the formed InP nanocrystals with the oxide shell.

Another interesting observation is that the addition of OA apparently influences the size distribution of the InP nanocrystals formed at 270 °C. As compared to a reaction without amine, we noted that the excitonic peak in the UV–vis absorption spectrum was much better defined when OA was added. This indicates that the amine molecules have potentially a second function in the studied reaction, namely the “activation” of P(TMS)₃. It has been reported that protic compounds such as alcohols and primary amines hydrolyse P(TMS)₃ and accelerate the formation of InP.¹⁵

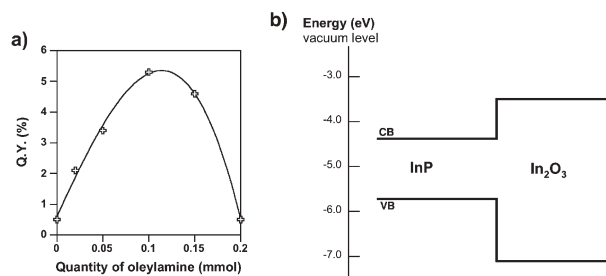


Fig. 4 a) Fluorescence Q.Y. as a function of the quantity of oleylamine initially added to the reaction mixture. b) Valence band (VB) and conduction band (CB) energy levels in InP¹³ and In₂O₃.¹⁴

Another example of “activation” by amine addition has been described in the synthesis of ZnSe nanocrystals.¹⁶

Finally, we checked the possibility of forming an oxide shell by simply introducing a small amount of air into the reaction flask during the growth of the nanocrystals. In this case, the X-ray diffraction pattern also shows the characteristic peaks of InP and In₂O₃.[†] While the width of the peaks corresponding to InP remained essentially unchanged, the peaks arising from In₂O₃ were narrower than before, resulting in a calculated crystallite size of 10.2 nm. The corresponding TEM micrograph showed that a mixture of 3 nm InP and rather polydisperse In₂O₃ nanoparticles of a mean size of 10 nm was formed. This demonstrates that the proposed method is a convenient and reliable way to form an In₂O₃ shell on InP nanocrystals, which cannot be obtained by the simple introduction of oxygen into the reaction medium.

To summarize, the novel core-shell system InP–In₂O₃ has been prepared by addition of a primary amine (OA) to the reaction mixture used for the synthesis of InP nanocrystals. The large bandgap of In₂O₃ (3.6 eV) and band offsets in the heterosystem with InP can provide an efficient confinement of both electrons and holes in the nanocrystal core (Fig. 4b). As a result, the thick oxide shell strongly enhances the fluorescence intensity and makes these nanocrystals suitable for applications such as biological labelling or light-emitting diodes. Amide formation and *in situ* generation of water most probably occur in a large variety of reactions involving the use of both carboxylic acid and primary amine stabilisers at high temperature. Therefore we suppose that this mechanism also plays an important role in the syntheses of other types of nanocrystals in which a combination of these stabilisers is used, such as for example FePt.¹⁷

Financial support from the French research ministry in the frame of “Action Concertée Nanoscience” (project NANOPTIP 2004-07) is gratefully acknowledged. Michaël Delalande is thanked for assistance with powder X-ray diffraction and one of the reviewers for helpful remarks concerning the reaction mechanism.

Notes and references

† The synthesis of InP nanocrystals was carried out under standard air-free techniques using the protocol reported in Ref. 3. Briefly, 0.1 mmol of indium(III) acetate, 0.3 mmol of myristic acid and 5 g of octadecene (ODE)

were loaded in a 50 mL three-necked flask. The mixture was degassed at 100 °C for 1 h in vacuum and then heated to 300 °C under argon flow. 0.05 mmol of tris(trimethylsilyl)phosphine, diluted with 2 g of ODE, were swiftly injected. The temperature was decreased to 270 °C for the growth of the nanocrystals, which was stopped after 10 minutes by removing the heating source. The nanocrystals were purified by addition of one equivalent of CH₃OH–CHCl₃ (1 : 1) and 10 equivalents of acetone, followed by centrifugation. For the synthesis of InP–In₂O₃ nanocrystals the same procedure is applied, except that 0.1 mmol of oleylamine were initially added to the indium precursor containing mixture and the injection/growth temperature was lowered to 270 °C.

‡ The lattice mismatch of bulk cubic InP and In₂O₃ accounts for ca. 14%.

- 1 O. I. Micic, H. M. Cheong, H. Fu, A. Zunger, J. R. Sprague, A. Mascarenhas and A. J. Nozik, *J. Phys. Chem. B*, 1997, **101**, 4904–4912.
- 2 D. V. Talapin, N. Gaponik, H. Borchert, A. L. Rogach, M. Haase and H. Weller, *J. Phys. Chem. B*, 2002, **106**, 12659–12663.
- 3 D. Battaglia and X. G. Peng, *Nano Lett.*, 2002, **2**, 1027–1030.
- 4 S. Xu, S. Kumar and T. Nann, *J. Am. Chem. Soc.*, 2006, **128**, 1054–1055.
- 5 M. A. Hines and P. Guyot-Sionnest, *J. Phys. Chem.*, 1996, **100**, 468–471; B. O. Dabbousi, J. RodriguezViejo, F. V. Mikulec, J. R. Heine, H. Mattoussi, R. Ober, K. F. Jensen and M. G. Bawendi, *J. Phys. Chem. B*, 1997, **101**, 9463–9475.
- 6 X. G. Peng, M. C. Schlamp, A. V. Kadavanich and A. P. Alivisatos, *J. Am. Chem. Soc.*, 1997, **119**, 7019–7029.
- 7 P. Reiss, J. Bleuse and A. Pron, *Nano Lett.*, 2002, **2**, 781–784.
- 8 S. Haubold, M. Haase, A. Kornowski and H. Weller, *ChemPhysChem*, 2001, **2**, 331–334.
- 9 O. I. Micic, B. B. Smith and A. J. Nozik, *J. Phys. Chem. B*, 2000, **104**, 12149–12156.
- 10 The synthesis of high quality InP nanocrystals was not possible at temperatures below 300 °C. Using temperatures above 270 °C for the preparation of InP–In₂O₃ nanocrystals is not possible in turn, as the In-containing precursor solution becomes turbid before injection of the phosphorus precursor.
- 11 A. A. Guzelian, J. E. B. Katari, A. V. Kadavanich, U. Banin, K. Hamad, E. Juban, A. P. Alivisatos, R. H. Wolters, C. C. Arnold and J. R. Heath, *J. Phys. Chem.*, 1996, **100**, 7212–7219.
- 12 W. S. Seo, H. H. Jo, K. Lee and J. T. Park, *Adv. Mater.*, 2003, **15**, 795–797.
- 13 A. Klein, *Appl. Phys. Lett.*, 2000, **77**(13), 2009–2011.
- 14 *Semiconductors and semimetals*, ed. R. K. Willardson and A. C. Beer, Academic Press, New York, 1966, vol. 2.
- 15 J. M. Nedeljkovic, O. I. Micic, S. P. Ahrenkiel, A. Miedaner and A. J. Nozik, *J. Am. Chem. Soc.*, 2004, **126**, 2632–2639.
- 16 L. S. Li, N. Pradhan, Y. Wang and X. Peng, *Nano Lett.*, 2004, **4**(11), 2261–2264.
- 17 S. H. Sun, C. B. Murray, D. Weller, L. Folks and A. Moser, *Science*, 2000, **287**, 1989–1992.